# Estimating seismic velocity variations in the Mississippi embayment from analysis of the ambient seismic field

Chunyu Liu[1], Khurram S. Aslam[1], and Eric G. Daub[2]

[1]University of Memphis
[2]Alan Turing Insitute

November 25, 2022

**Abstract**

We use cross-correlation of the ambient seismic field to estimate seasonal variations of seismic velocity in the Mississippi Embayment and to determine the underlying physical mechanisms. Our main observation is that the [?]t/t variations correlate primarily with the water table fluctuation, with the largest positive value from May to July and the largest negative value in September/October relative to the annual mean. The correlation coefficients between water table fluctuation and [?]t/t are independent of the interstation distance and frequency, but high coefficients are observed more often in the 0.3-1 Hz than 1-2 Hz because high-frequency coherent signals attenuate faster than low-frequency ones. The [?]t/t variations lag behind the water table fluctuation by about 20 days, which suggests the velocity changes can be attributed to the pore pressure diffusion effect. The maximum [?]t/t variations decrease with frequency from 0.03% at 0.3-1 Hz to 0.02% at 1-2 Hz, and the differences between them might be related to different local sources or incident angles. The seasonal variations of [?]t/t are azimuthally independent, and a large increase of noise amplitude only introduces a small increase to the [?]t/t variation. At close distances, the maximum [?]t/t holds a wide range of values, which is likely related to local structure. At larger distances, velocity variations sample a larger region so that it stabilizes to a more uniform value. We find that the observed changes in wave speed are in agreement with the prediction of a poroelastic model.

# Estimating seismic velocity variations in the Mississippi embayment from analysis of the ambient seismic field

Chunyu Liu,[1] Khurram S. Aslam,[1,3] Eric G. Daub[1,2]

**Key Points:**

- We observe the minimum wave speed from May to July due to the increased pore pressure from the water table fluctuation and the maximum wave speed in September/October.
- The $\delta t/t$ correlates primarily with the water table fluctuation and does not show an obvious relationship with the atmospheric pressure, temperature, precipitation, and wind speed.
- A poroelastic model can explain the velocity variations in the crust.

Corresponding author: Chunyu Liu (yclmq3@mst.edu)

[1]Center for Earthquake Research and Information, University of Memphis, Memphis, Tennessee, USA.

[2]Alan Turing Institute, London, UK

[3]University of Oregon, Oregon, USA

**Abstract.**

We use cross-correlation of the ambient seismic field to estimate seasonal variations of seismic velocity in the Mississippi Embayment and to determine the underlying physical mechanisms. Our main observation is that the $\delta t/t$ variations correlate primarily with the water table fluctuation, with the largest positive value from May to July and the largest negative value in September/October relative to the annual mean. The correlation coefficients between water table fluctuation and $\delta t/t$ are independent of the interstation distance and frequency, but high coefficients are observed more often in the 0.3-1 Hz than 1-2 Hz because high-frequency coherent signals attenuate faster than low-frequency ones. The $\delta t/t$ variations lag behind the water table fluctuation by about 20 days, which suggests the velocity changes can be attributed to the pore pressure diffusion effect. The maximum $\delta t/t$ variations decrease with frequency from 0.03% at 0.3-1 Hz to 0.02% at 1-2 Hz, and the differences between them might be related to different local sources or incident angles. The seasonal variations of $\delta t/t$ are azimuthally independent, and a large increase of noise amplitude only introduces a small increase to the $\delta t/t$ variation. At close distances, the maximum $\delta t/t$ holds a wide range of values, which is likely related to local structure. At larger distances, velocity variations sample a larger region so that it stabilizes to a more uniform value. We find that the observed changes in wave speed are in agreement with the prediction of a poroelastic model.

## 1. Introduction

Extensive field and laboratory studies have been dedicated to understanding the crustal responses including seismic velocity variations and subsurface strain changes due to the internal tectonic and external climatological stress loadings [*Hadziioannou et al.*, 2009; *Ben-Zion and Allam*, 2013; *Ben-Zion and Leary*, 1986; *Sens-Schönfelder and Larose*, 2008; *Meier et al.*, 2010; *Hillers et al.*, 2015a; *Wu et al.*, 2016; *De Fazio et al.*, 1973]. Monitoring the crustal response can not only track the evolving stress and constrain the effective rheology with depth, but can also help to understand the crustal response to the internal tectonic stress by removing the response to the climatological stress loadings [*Hillers et al.*, 2015a; *Rivet et al.*, 2015; *Wang et al.*, 2017]. Because different rocks or structures respond differently to the internal and external loadings, monitoring the crustal response can also help to identify local structure anomalies and understand wave propagation and attenuation [*Wang et al.*, 2017]. More specifically, measurements of the temporal changes of seismic velocity can shed light on the fault zone coseismic damage and postseismic healing [*Wu et al.*, 2016; *Liu et al.*, 2018b; *Brenguier et al.*, 2008a], volcanic eruption early warning [*Duputel et al.*, 2009; *Brenguier et al.*, 2008b], groundwater levels [*Clements and Denolle*, 2018], climatological parameters such as precipitation [*Sens-Schönfelder and Wegler*, 2006], temperature [*Meier et al.*, 2010; *Sens-Schönfelder and Larose*, 2008], and atmospheric pressure [*Niu et al.*, 2008; *Silver et al.*, 2007], solid earth tidal [*De Fazio et al.*, 1973] and oceanic tidal deformation [*Hillers et al.*, 2015b; *Yamamura et al.*, 2003], and instrumental errors [*Sens-Schönfelder*, 2008; *Stehly et al.*, 2007]. Taking advantage of long-term dense seismic station deployments, a systematic investigation of seismic velocity variation can improve our understanding of the crustal response to the climatological loadings.

The Mississippi embayment (ME) (Fig. 1) is a SSW plunging trough filled with late Cretaceous and Cenozoic sediments that can reach a thickness of approximately 1.5 km [*Hildenbrand and Hendricks*, 1995; *Dart*, 1992; *Dart and Swolfs*, 1998]. The ME has experienced long-term and complicated geological activities including uplift, rifting and subsidence, and has hosted three $M_w > 7.0$ earthquakes (Fig. 1) that occurred in the winter of 1811 - 1812 [*Johnston and Schweig*, 1996]. We target the ME for two reasons. First, long-term continuous monitoring and dense broadband station distribution allow us to conduct a thorough temporal velocity investigation which may provide insight into how the climatological parameters influence the seismic velocity. Secondly, few studies of this type have been done in intraplate fault zones, so such an investigation can help us understand if there are significant differences between interplate and intraplate fault zones and how they respond to external changes in forcing.

Estimating seismic velocity change has been done by measuring the travel time or phase difference from active sources including explosions [*Li et al.*, 1998, 2003, 2006; *Nishimura et al.*, 2000], airguns [*Wegler et al.*, 2006] and repeating earthquakes [*Poupinet et al.*, 1984; *Peng and Ben-Zion*, 2006; *Rubinstein and Beroza*, 2004a, b; *Rubinstein et al.*, 2007; *Schaff and Beroza*, 2004], and by computing the dephasing of the ambient noise cross-correlations (CCs) [*Sens-Schönfelder and Wegler*, 2006; *Brenguier et al.*, 2008a] or auto-correlations (ACs) [*Minato et al.*, 2012; *Ohmi et al.*, 2008]. We prefer ambient noise analysis because it not only circumvents the uncertainty of repeating earthquakes and high expense of the active sources but also allows for long-term velocity monitoring over time periods of months to years. The CCs of the ambient noise can effectively retrieve empirical Green's function between a pair of stations [*Shapiro and Campillo*, 2004; *Sabra et al.*, 2005; *Weaver and Lobkis*, 2001; *Derode et al.*, 2003]. The dephasing of scattered waves in daily CCs relative to those in a reference CC reflects the temporal change of the elastic behavior of the crust.

We apply ambient noise CCs to all broadband seismic stations inside the ME over four frequency ranges, and investigate temporal variations of seismic velocity and correlation with the climatological parameters. We compare the calculated seismic velocity variation of each station pair with the regional climatological parameters to investigate the possible mechanisms for the velocity changes. We address the following questions: what are the physical mechanisms behind the temporal velocity changes in the ME? Do the maximum velocity variations depend on characteristics of the waves, such as the frequency, inter-station distance and azimuth? What are the correlation coefficients of velocity changes with the climatological parameter variations? The cross-correlation methods applied to the data from the ME give us a unique view into the physical mechanisms behind changes in seismic velocity over time and how the changes are related to the non-tectonic effects that may complicate the analysis of more active tectonic regions.

## 2. Data and analysis procedure

The installation of Northern Embayment Lithosphere Experiment (NELE) with large aperture and continuous recording in 2014 enables us to investigate the temporal variations of seismic velocity. We use 53 broadband stations (Fig. 1) to compute the CCs. All broadband stations are inside the ME as can be seen by comparing station locations to the sediment thickness contours. Because sediment-influenced waves may better reflect the sediment elastic behavior than the direct crustal surface wave arrivals, we limit the interstation distance to be 100 km where *Langston et al.* [2005] and *Liu et al.* [2019] observed direct sedimentary surface wave arrivals in the passband of 0.2-1.5 Hz. In order to investigate the annual temporal variations, we only use stations which have a continuous full-year recording in 2014. Finally, we compute 373 velocity variations for all station pairs in 2014 to investigate how they behave seasonally.

We follow the analysis procedure of *Brenguier et al.* [2008a] and *Lecocq et al.* [2014] in this study. We download continuous daily vertical component miniseed data from IRIS (www.iris.edu) by the FDSN web service, and use the MSNoise Python package [*Lecocq et al.*, 2014] to compute the CCs. The data processing details are available in *Lecocq et al.* [2014], and are described briefly here. For each station pair, we first scan yearly data into MSNoise, down-sample to 5 Hz, and remove instrument response. We also remove earthquakes by the root-mean-square (RMS) temporal normalization, and reduce the effect of non-uniform source distributions by spectral whitening. *Langston et al.* [2009] and *Liu et al.* [2018a] observed the major oceanic-generated ambient noise in the frequency range of 0.02 - 0.33 Hz in the ME, and sedimentary surface waves emerge in the passband of 0.2 - 1.5 Hz [*Langston et al.*, 2005; *Liu et al.*, 2019]. Considering the dominant frequency range of waves scattered by sediments is higher than that of the oceanic ambient noise [*Liu et al.*, 2019], we define 4 frequency ranges: 0.3 - 1 Hz, 0.5 - 1.2 Hz, 0.7 - 1.5 Hz, and 1 - 2 Hz. Because Rayleigh waves have peak sensitivity to the shear wave velocity changes at the depth of 1/3 of a wavelength, scattered waves with a period of 3 s and phase velocity of 1.7 km/s [*Dorman and Smalley*, 1994] can be sensitive to velocity changes at depths up to 1.7 km. We stack -15 and +15 days for a monthly CC on the selected date, and average all daily CCs to obtain the reference CC. We use a moving-window cross-spectral (MWCS) method [*Poupinet et al.*, 1984; *Clarke et al.*, 2011] to measure the relative dephasing between monthly moving stack CCs and yearly reference CC, as *Zhan et al.* [2013] suggested that the stretching method [*Wegler and Sens-Schönfelder*, 2007] can cause apparent velocity changes due to changes in the amplitude and phase spectrum. The MWCS measures the arrival time difference between two windowed waveforms by computing cross-coherency between energy densities in the frequency domain. Linear regression of time differences over moving coda windows constrains the fractional change in travel time $\delta t/t$. The errors of $\delta t/t$ are estimated using the cross-coherency and the squared misfit to the linear regression slope [*Clarke et al.*, 2011]. The velocity change ($\delta v/v$) is deduced by the relationship $\delta v/v$ = - $\delta t/t$, which assumes that the $\delta v/v$ is spatially homogeneous. A coda window defined for the MWCS is shown in Fig. 2. We define the coda window based on the timing of large amplitude scattered wave arrivals (group velocity $<$ 1.0 km/s) in the monthly moving stack CCs (Fig. 2).

The velocity variations are known to be associated with climatological parameters such as water table, precipitation, temperature, atmospheric pressure, and wind speed [*Hillers et al.*, 2015a; *Meier et al.*, 2010; *Sens-Schönfelder and Wegler*, 2006; *Sens-Schönfelder and Larose*, 2008]. We obtain daily water table data of 11 stations from the USGS water information system and precipitation, temperature, atmospheric pressure, and wind speed from the National Oceanic and Atmospheric Administration (NOAA). We calculate the water table fluctuation by subtracting the daily water table from the maximum water table over one year. Because the velocity variations have a different dependence on the changes of the climatological parameters, we remove the mean and normalize the maximum of the absolute value of the velocity variations, water table fluctuation, precipitation, temperature, atmospheric pressure and wind speed to unity for comparison.

## 3. Analysis of seismic velocity variations

We measure yearly $\delta t/t$ variations for all 373 station pairs over 4 predefined frequency ranges in 2014. The CCs for all station pairs are computed in the passband of 0.3 - 2 Hz, and the MWCS and $\delta t/t$ variations are determined in predefined frequency ranges. The $\delta t/t$ increases to its maximum in May and June and decreases to its minimum in September and October relative to the average (Fig. 3). The $\delta t/t$ variations correlate primarily with the normalized water table fluctuation in the four predefined frequency ranges. We select 205, 198, 158, and 96 $\delta t/t$ variations in the passbands of 0.3-1 Hz, 0.5-1.2 Hz, 0.7-1.5 Hz, and 1-2 Hz based on two criteria: 1) the correlation coefficient with the normalized water table fluctuation is higher than 0.3, and 2) they show seasonal variation. That is, the wave speed is slower than average in late spring to summer and is faster in late fall to early winter. If we cannot observe a seasonal variation of $\delta t/t$, estimation of maximum $\delta t/t$ cannot be correctly determined. We determine the maximum $\delta t/t$ for each station pair by smoothing the $\delta t/t$ over entire year with a 10-day moving average window and compute the maximum of the smoothed variations, which removes spurious velocity variations with large errors. In the following sections, we evaluate how the $\delta t/t$ and correlation coefficients vary in different frequency ranges, how the maximum $\delta t/t$ and correlation coefficients depend on the characteristics of the waves, such as interstation distance and azimuth.

### 3.1. Correlation with the climatological parameters

Climatological loadings can induce various crustal responses including stress/strain changes [*Ben-Zion and Allam*, 2013], earthquake triggering [*Liu et al.*, 2009; *Husen et al.*, 2007], and seismic velocity variations [*Hillers et al.*, 2015b; *Meier et al.*, 2010]. The precipitation/water table fluctuation, atmospheric pressure, wind speed influence the elastic stress by changing the pore pressure or water saturation, air pressure redistribution, and wind on contact shearing, respectively. The temperature has an impact on regional thermoelastic stress because of thermal expansion or contraction due to ambient temperature changes. The elastic and thermoelastic stress changes directly affect the strain field, which can be used to model the seismic velocity variations [*Tsai*, 2011; *Wang et al.*, 2017].

The magnitude of the velocity variations and their dependence on the climatological parameters vary throughout the world. *Sens-Schönfelder and Wegler* [2006] observed that the $\delta v/v$ varies seasonally with an amplitude of 0.02% in the frequency band $> 0.5$ Hz at Merapi volcano, Indonesia, and suggested that the variation is due to changes of the water table. *Wang et al.* [2017] observed up to a 0.02% velocity variation in the passband of 0.15-0.9 Hz using data from 2011 to 2012 throughout Japan, and proposed that the velocity variations could be due to different effects including pore pressure, snow depth, and sea level changes for different regions. *Ben-Zion and Leary* [1986] suggested the temperature could cause an effect 10 times larger than water table fluctuations around 15 m. *Meier et al.* [2010] observed a maximum 0.1% velocity change in the 0.1-2 Hz passband using data from 2001 to 2004 in the Los Angeles basin, and suggested that it was associated with the thermoelastic strain variation. These studies indicate that the velocity variations could be associated with different climatological parameters and maximum velocity variations induced by temperature could be higher than that caused by water table fluctuations.

Determining the magnitude of velocity variation and its most strongly correlated parameter can help us understand the dominant mechanisms driving the velocity changes for the ME. In Fig. 3, we show the correlations between the normalized average $\delta t/t$ for all station pairs and the normalized precipitation, water table fluctuation, temperature, atmospheric pressure and wind speed in four predefined frequency ranges. The $\delta t/t$ correlates most strongly with the normalized water table fluctuation. We use a physical model (Fig. 4) to explain the observed velocity variations in the following section. Atmospheric pressure, precipitation and wind speed do not show any clear correlation with the $\delta t/t$ observations. In Fig. 5, average maximum velocity variations for all station pairs range from 0.02% to 0.05% in different frequency bands, and are similar in magnitude to the changes for Japan and for Merapi volcano.

The strong correlation between $\delta t/t$ and the water table fluctuation could be due to two possible effects. The water table fluctuation can affect the direct hydrological and poroelastic strain, which are related to the direct water loading and water diffusion effect, respectively. The maximum velocity variations due to the direct hydrological elastic or poroelastic strain changes are around 0.04% for the Los Angeles basin [*Tsai*, 2011]. With similar sedimentary rock types and a few meters fluctuation in the water table, we might expect a similar magnitude of velocity variation for the ME. Direct water loading can affect hydrological strain instantaneously, but water diffusion usually take some time to influence poroelastic strain. Direct water loading increases $\delta v/v$ through an increase of water saturation at shallow depth while water diffusion increases pore pressure and decreases the area of grain contact, which decreases the $\delta v/v$ at deeper levels. The $\delta t/t$ changes show a delay of 20 days relative to the normalized water table fluctuation based on when the maximum and minimum values occur (Fig. 3). Our observations suggest that the water diffusion effect is the dominant mechanism for the velocity changes.

As *Tsai* [2011] and *Ben-Zion and Leary* [1986] modeled, the temperature is positively correlated with the $\delta v/v$. *Hillers et al.* [2015a] also observed that the $\delta v/v$ from 0.1 to 8 Hz increased to its maximum in July for the San Jacinto fault area, and the $\delta v/v$ variations lag behind the temperature by about one month. In the ME, the $\delta v/v$ variations are negatively correlated with temperature changes (Fig. 3), which is opposite to what would be expected based on previous results. Based on this, we suggest that the temperature changes might not have an effect on velocity variations in the ME. Strong wind energy is usually in a higher frequency range than the predefined passbands in this study [*Withers et al.*, 1996; *Hillers et al.*, 2015a]. Because wind forces should affect the elastic stress instantaneously, the velocity variations are not likely to be related to the changes of the wind speed. How the climatological parameters interact with each other and if that interaction could affect the velocity variation is not considered in this study.

### 3.2. A poroelastic physical model for seismc velocity changes

To facilitate our understanding of the dominant mechanism in the ME, we use a poroelastic physical model to estimate seasonal velocity variations from 2010 to 2018. An approximate time-dependent poroelastic solution from *Tsai* [2011] is:

$$A(t) = \frac{1+\nu}{1-\nu}\frac{\alpha p_0(1-2\nu)}{E}\sqrt{\hat{k_{hy}}}cos(\omega t - \frac{cot^{-1}\hat{k_{hy}}}{2}), \quad (1)$$

in which $A(t)$ is time-dependent strain amplitude on the surface, $\nu$ is Possion's ratio, $p_0$ is the amplitude of pore pressure variations, Biot-Willis coefficient $\alpha$ is defined as $\alpha = 1 - C_s/C_d$ where $C_s$ is unjacketed bulk compressibility and $C_d$ is drained bulk compressibility [*Biot and Willis*, 1957], $E$ is Young's modulus, $\omega$ is equal to $2\pi/T$ where $T$ is the period of water table fluctuation, $\hat{k_{hy}}$ is a normalized hydraulic diffusivity and is equal to $k_{hy}k^2/\omega$, $k$ is equal to $2\pi/\lambda$ with $\lambda$ to be related to the dominant wavelength of local topography, and $k_{hy}$ is hydraulic diffusivity.

We estimate the normalized diffusivity $\hat{k_{hy}}$ close to 1 from the relationship of delay time $dt$ (22 days) and $\hat{k_{hy}}$, $dt = cot^{-1}\hat{k_{hy}}/2\omega$ [*Tsai*, 2011]. *Catchings* [1999] suggested the Possion ratio $\nu$ to be 0.3. We fit a simple sinusoidal function to estimate the amplitude ($h = 1.6$ m) of water table flutuation (Fig. 4(A)), and compute a pore pressure variation $p_0$ as $\rho g h = 1.6 \times 10^4$ Pa. An approximate Young's modulus for sandstone [*Detournay and Cheng*, 1993] is $1.6 \times 10^{10}$ Pa. An experimental study on $C_s$ and $C_d$ from *Hart* [2000] suggested that $\alpha$ ranges from 0.6 to 0.9 for sandstone. We use $\alpha = 0.7$ which is the same as the value used in *Tsai* [2011] for the following model.

Using the time-dependent water table fluctuation and Eq. (1), we can estimate the maximum strain amplitude to be of the order of $10^{-7}$. Seasonal velocity variations can also be roughly estimated by $\delta v/v = m/\mu A(t)(1 - 2\nu)$, in which $\mu$ is the second Lamé constant and $m$ is the Murnaghan constant [*Murnaghan*, 1951; *Hughes and Kelly*, 1953; *D'Angelo et al.*, 2008]. Lab experiments suggest that $m/\mu$ can range from -1000 to -200 for sandstone [*D'Angelo et al.*, 2008]. We compute seasonal variations of velocity for 43 pairs of stations from 2010 to 2018, and average over them to obtain an observed velocity change in the passband of 0.3 - 1 Hz (Fig. 4(B)). An approximate $m/\mu$ value required to match the modeled $\delta v/v$ with the observed one is -2000. *Tsai* [2011] also found a similar value to match velocity variations in the Los Angeles basin, and emphasized that the Murnaghan constant should be better characterized for relevant materials to obtain an accurate quantitative comparison.

### 3.3. $\delta t/t$ in different frequency ranges

Exploring velocity variations in different frequency bands can shed light on the depth sensitivity of the velocity variations and its dependence on frequency. Regardless of the velocity dependence on distance, we average all $\delta t/t$ variations in the 0.3-1 Hz, 0.5-1.2 Hz, 0.7-1.5 Hz, and 1-2 Hz frequency bands and observe that the velocity is lower than average in May and June and higher in September and October (Fig. 5(A)). Average maximum $\delta t/t$ decreases with frequency from 0.03% at 0.3-1 Hz to 0.02% at 1-2 Hz. *Meier et al.* [2010] also observed the maximum $\delta t/t$ decreases from 0.5% at 0.1-0.2 Hz to 0.2% at 0.1-1 and 0.5-2 Hz in the Los Angles basin. *Hillers et al.* [2015a] observed a peak-to-peak velocity change from 0.4-0.8% at 0.1-0.4 Hz to 0.1% at 1-4 Hz in the San Jacinto fault area. One possible explanation is that the scattered waves in different frequency ranges are induced by the ME basin edges [*Kawase*, 1996; *Liu et al.*, 2018a; *Liu et al.*, 2019] and could be associated with different local sources or different incidence angles [*Tanimoto et al.*, 2006; *Froment et al.*, 2010; *Weaver et al.*, 2009]. The noise from different local sources or with different incidence angles might induce different effects on the velocity. To confirm that the averaged $\delta t/t$ variations in different frequency ranges are not biased by the non-uniform interstation distance distribution, we separate station pairs into 0-30, 30-60, 60-100 km groups. Across these groups, we find that the maximum $\delta t/t$ decreases with the increasing frequency and the peak/trough pattern does not change with distance (Fig. 5).

### 3.4. $\delta t/t$ dependence on the interstation azimuth and noise amplitude

Seasonal variation of seismic velocity can reflect changes in material properties or be induced by seasonal changes of noise amplitude [*Hillers et al.*, 2015a]. Heterogeneous distributions of the noise source can bias the estimation of arrival time [*Weaver et al.*, 2009; *Froment et al.*, 2010]. Thus, a long-term change in the noise source distribution over several months also be the cause of spurious seismic velocity changes.

Sources of microseisms usually distribute non-uniformly in different seasons [*Young*, 1999; *Tian and Ritzwoller*, 2015; *Langston et al.*, 2009; *Liu et al.*, 2019]. However, scattering by local structures can randomize propagation directions and increase isotropy. In the ME, *Liu et al.* [2019] suggested that the generation of sedimentary surface waves in the passband of 0.2-1 Hz might be related to the basin edges. In the coda window, scattered waves (group velocity $<$ 1 km/s) can be composed of sedimentary surface waves (group velocity 0.7 m/s). In order to investigate if the velocity variations are azimuthally dependent, we compare the average velocity variations using station pairs with different azimuths. We initially do not differentiate the positive and negative lags of the CCs while calculating the $\delta t/t$ variations, so the propagation direction of scattered waves corresponding to the $\delta t/t$ estimation is uncertain. Because the edge of the ME surrounds the stations on the northwest and northeast (Fig. 1) and the edge of the embayment might be related to the generation of scattered waves, we use 0° - 90° and 270° - 360° as azimuths of possible noise sources. We compute the average $\delta t/t$ variations from all station pairs with the azimuth in these ranges. In Fig. 6, the average $\delta t/t$ variations are similar to each other, and the difference between them are very small compared to the maximum seasonal variations of the average $\delta t/t$. *Hadziioannou et al.* [2011] also observed that changes in noise directions do not influence the $\delta t/t$ measurements significantly. We conclude that the non-uniform distribution of noise sources has a small effect on the $\delta t/t$ variations.

The amplitude of the ambient noise usually shows seasonal variations [*Stehly et al.*, 2006; *Yang et al.*, 2007; *Young*, 1999]. To investigate the velocity variation dependence on the seasonal changes of the amplitude of noise sources, we compare the $\delta t/t$ variations with the seasonal variations of the daily noise amplitude. We estimate hourly noise amplitude by averaging the absolute value of original data in the passband of 0.3-2 Hz, and determine the daily noise amplitude by averaging over 24 hours. In Fig. 7, we observe high amplitude from November to May and low amplitude from June to October, which is consistent with the generally observed high noise energy during winter in the northern hemisphere [*Hillers et al.*, 2015a; *Young*, 1999; *Liu et al.*, 2019]. We also observe high similarity between seasonal variation of the wind speed and average noise amplitude. *Hillers et al.* [2015a] suggested the low-frequency (0.1-2 Hz) noise in the San Jacinto fault area can be excited by the atmosphere-ocean-lithosphere interactions. Thus, ambient noise from 0.3 to 2 Hz in the ME can be composed of oceanic microseisms [*Langston et al.*, 2005, 2009; *Liu et al.*, 2018a], induced surface waves at the basin-edges [*Kawase*, 1996; *Liu et al.*, 2018a; *Liu et al.*, 2019], and wind. In Fig. 7, we compare the variations of noise amplitude and $\delta t/t$ measurements from January to April and October to December, and observe high similarity between them. We also observe a small increase of $\delta t/t$ measurements with a large increase of noise amplitude in November (Fig. 7). *Hillers et al.* [2015a] also proposed that changes in noise amplitude do not affect the velocity directly but can introduce a bias, a small increase or decrease, in the $\delta t/t$ measurements. Even if a decrease of noise amplitude from April to September can induce a small decrease of the $\delta t/t$ measurement, the decrease is relatively small compared to the $\delta t/t$ changes induced from the water table fluctuations. We conclude that the velocity variations are most likely related to the pore pressure changes in the crust or sediments, rather than changes due to the seasonal variations of the ambient noise amplitude.

### 3.5. Maximum $\delta t/t$ and correlation coefficient as a function of interstation distance

In order to investigate propagation properties of noise in the sediments, we explore the relationship between $\delta t/t$ and interstation distance. The maximum $\delta t/t$ decreases non-linearly with the increasing interstation distance as shown in Fig. 8(A). Because there are not enough station pairs with the interstation distance from 0 to 15 km, our analysis of the relationship between the $\delta t/t$ and distance is limited to 15-100 km. *Meier et al.* [2010] also observed that seasonal variations of $\delta t/t$ became weaker and finally disappeared when the interstation distance is greater than 60 km. They suggested that the vanishing of seasonal variation of $\delta t/t$ is due to absence of coherent noise in the coda window. At close distances, the $\delta t/t$ holds a wide range of values, which could be associated with greater localized variations in $\delta t/t$ in the local sediment structure. At larger distances, $\delta t/t$ variations tend to stabilize to a narrow range.

We compute correlation coefficients between normalized $\delta t/t$ variations and the normalized water table fluctuation over different distances, and investigate how the correlation coefficients depend on the interstation distance and frequency (Fig. 8(B)). The correlation coefficients are independent of the interstation distance or frequency, but high coefficients

(> 0.6 ) are observed more often in the 0.3-1 Hz than 1-2 Hz passband because high-frequency coherent signals attenuate faster than low-frequency ones (Fig. 8(B)).

## 4. Conclusions

We apply ambient noise correlation to 53 broadband stations which have continuous recordings in 2014, and analyze the seasonal variations of seismic velocity and determine how they correlate with the climatological parameters. We observe maximum $\delta t/t$ in May and June and minimum $\delta t/t$ in September and October relative to the average. The maximum $\delta t/t$ decreases with the frequency from 0.03% in the passband of 0.3-1 Hz to 0.02% in the 1-2 Hz. Scattered waves from different local sources or with different incident angles might induce different seismic velocity changes in the predefined frequency ranges. At close distances, the maximum $\delta t/t$ holds a wide range of values, which could be associated with the local sediment structure. At larger distances, velocity variations tend to stabilize to an average value. The average $\delta t/t$ variations for station pairs with different azimuths are similar to each other, which suggests that the velocity variations do not depend on the azimuthal distribution of noise sources. Seasonal variations of noise amplitude might introduce a bias into the $\delta t/t$ estimation but the bias is small compared to the large velocity variations induced by the water table fluctuation.

The $\delta t/t$ correlates primarily with the normalized water table fluctuation and does not show an obvious relationship with the atmospheric pressure, temperature, precipitation or wind speed. The $\delta t/t$ variation lags behind the water table fluctuation about 20 days, which suggests the water diffusion effect is the dominant mechanism for the velocity change. We use a poroelastic model to estimate seasonal variations of $\delta v/v$ from 2010 to 2018. That is, elastic wave speeds can be estimated from strain amplitude in the strain energy function [*Murnaghan*, 1951]. The observed value of $\delta v/v$ require $m/\mu$ with value around -2000, which is close to values from lab experiments, from -200 to -1000 [*D'Angelo et al.*, 2008]. The correlation coefficients between the water table fluctuation and $\delta t/t$ are independent of the interstation distance and frequency, but more high coefficients (>0.6) are observed in the passband of 0.3-1 Hz than 1-2 Hz. One possible explanation could be that high-frequency coherent signals attenuate faster than low-frequency ones.

The results of the poroelastic model suggest that ambient noise cross-correlations can be used to estimate the hydrological properties of sediments in other regions based on the observed delay between the water table fluctuations and seismic velocity changes. This can provide an independent estimate of soil properties that are used in groundwater flow models. Additionally, our results confirm that the first order correction to the elastic properties of soils in the ME are consistent with other laboratory and seismic studies and could be related to the strain induced by the poroelastic diffusion.

Our results confirm that climatological variations play a role in determining the elastic properties of sediments in the Central and Eastern United States. Future studies should be completed in other intraplate regions to examine if similar behavior is found, which would provide additional ways to understand the physical mechanisms behind wave propagation and the temporal response of the crust to external forcing. In this manner, we can better determine if temporal velocity changes can be related to stress accumulation on faults due to tectonic loading and improve our ability to determine earthquake risk in intraplate fault regions.

**Acknowledgments.** This work was supported by funding from DOE Office of Basic Energy Science, Geoscience Program through Los Alamos National Laboratory and the

Center for Earthquake Research and Information (CERI), the University of Memphis. The ground water table data is provided from the USGS water resources information system (www.waterdata.usgs.gov), and the precipitation, temperature, atmospheric pressure and the wind speed data is from the National Oceanic and Atomospheric Administration (NOAA) (www.noaa.gov).

## References

Ben-Zion, Y., and A. Allam (2013), Seasonal thermoelastic strain and postseismic effects in Parkfield borehole dilatometers, *Earth and Planetary Science Letters*, *379*, 120–126.

Ben-Zion, Y., and P. Leary (1986), Thermoelastic strain in a half-space covered by unconsolidated material, *Bulletin of the Seismological Society of America*, *76*(5), 1447–1460.

Biot, M. A., and D. Willis (1957), The elastic coeff cients of the theory of consolidation, *J. appl. Mech*, *24*, 594–601.

Brenguier, F., M. Campillo, C. Hadziioannou, N. Shapiro, R. M. Nadeau, and E. Larose (2008a), Postseismic relaxation along the san andreas fault at Parkfield from continuous seismological observations, *Science*, *321*(5895), 1478–1481.

Brenguier, F., N. M. Shapiro, M. Campillo, V. Ferrazzini, Z. Duputel, O. Coutant, and A. Nercessian (2008b), Towards forecasting volcanic eruptions using seismic noise, *Nature Geoscience*, *1*(2), 126.

Catchings, R. (1999), Regional vp, vs, vp/vs, and poisson's ratios across earthquake source zones from memphis, tennessee, to st. louis, missouri, *Bulletin of the Seismological Society of America*, *89*(6), 1591–1605.

Clarke, D., L. Zaccarelli, N. Shapiro, and F. Brenguier (2011), Assessment of resolution and accuracy of the Moving Window Cross Spectral technique for monitoring crustal temporal variations using ambient seismic noise, *Geophysical Journal International*, *186*(2), 867–882.

Clements, T., and M. A. Denolle (2018), Tracking groundwater levels using the ambient seismic field, *Geophysical Research Letters*.

D'Angelo, R., K. Winkler, and D. Johnson (2008), Three wave mixing test of hyperelasticity in highly nonlinear solids: Sedimentary rocks, *The Journal of the Acoustical Society of America*, *123*(2), 622–639.

Dart, R. L. (1992), Catalog of pre-Cretaceous geologic drill-hole data from the upper Mississippi Embayment; a revision and update of open-file report 90-260, *Tech. rep.*, US Dept. of the Interior, US Geological Survey,.

Dart, R. L., and H. S. Swolfs (1998), Contour mapping of relic structures in the Precambrian basement of the Reelfoot rift, North American midcontinent, *Tectonics*, *17*(2), 235–249.

De Fazio, T. L., K. Aki, and J. Alba (1973), Solid earth tide and observed change in the in situ seismic velocity, *Journal of Geophysical Research*, *78*(8), 1319–1322.

Derode, A., E. Larose, M. Campillo, and M. Fink (2003), How to estimate the Green's function of a heterogeneous medium between two passive sensors? Application to acoustic waves, *Applied Physics Letters*, *83*(15), 3054–3056.

Detournay, E., and H. D. Cheng (1993), Fundamentals of poroelaticity in comprehensive rock engineering: Principles, practice and projects, *2*.

Dorman, J., and R. Smalley (1994), Low-frequency seismic surface waves in the upper mississippi embayment, *Seismological Research Letters*, *65*(2), 137–148.

Duputel, Z., V. Ferrazzini, F. Brenguier, N. Shapiro, M. Campillo, and A. Nercessian (2009), Real time monitoring of relative velocity changes using ambient seismic noise at the Piton de la Fournaise volcano (La Réunion) from January 2006 to June 2007, *Journal of Volcanology and Geothermal Research*, *184*(1-2), 164–173.

Froment, B., M. Campillo, P. Roux, P. Gouedard, A. Verdel, and R. L. Weaver (2010), Estimation of the effect of nonisotropically distributed energy on the apparent arrival time in correlations, *Geophysics*, *75*(5), SA85–SA93.

Hadziioannou, C., E. Larose, O. Coutant, P. Roux, and M. Campillo (2009), Stability of monitoring weak changes in multiply scattering media with ambient noise correlation: Laboratory experiments, *The Journal of the Acoustical Society of America*, *125*(6), 3688–3695.

Hadziioannou, C., E. Larose, A. Baig, P. Roux, and M. Campillo (2011), Improving temporal resolution in ambient noise monitoring of seismic wave speed, *Journal of Geophysical Research: Solid Earth*, *116*(B7).

Hart, D. J. (2000), *Laboratory measurements of poroelastic constants and flow parameters and some associated phenomena*, P.h.D thesis, University of Wisconsin–Madison.

Hildenbrand, T. G., and J. D. Hendricks (1995), Geophysical setting of the Reelfoot rift and relations between rift structures and the New Madrid seismic zone, *Tech. rep.*

Hillers, G., Y. Ben-Zion, M. Campillo, and D. Zigone (2015a), Seasonal variations of seismic velocities in the San Jacinto fault area observed with ambient seismic noise, *Geophysical Journal International*, *202*(2), 920–932.

Hillers, G., L. Retailleau, M. Campillo, A. Inbal, J.-P. Ampuero, and T. Nishimura (2015b), In situ observations of velocity changes in response to tidal deformation from analysis of the high-frequency ambient wavefield, *Journal of Geophysical Research: Solid Earth*, *120*(1), 210–225.

Hughes, D. S., and J. Kelly (1953), Second-order elastic deformation of solids, *Physical review*, *92*(5), 1145.

Husen, S., C. Bachmann, and D. Giardini (2007), Locally triggered seismicity in the central Swiss Alps following the large rainfall event of August 2005, *Geophysical Journal International*, *171*(3), 1126–1134.

Johnston, A. C., and E. S. Schweig (1996), The enigma of the new madrid earthquakes of 1811–1812, *Annual Review of Earth and Planetary Sciences*, *24*(1), 339–384.

Kawase, H. (1996), The cause of the damage belt in kobe:the basin-edge effect, constructive interference of the direct s-wave with the basin-induced diffracted/rayleigh waves, *Seismological Research Letters*, *67*(5), 25–34.

Langston, C. A., P. Bodin, C. Powell, M. Withers, S. Horton, and W. Mooney (2005), Bulk sediment $Q_p$ and $Q_s$ in the Mississippi Embayment, central United States, *Bulletin of the Seismological Society of America*, *95*(6), 2162–2179.

Langston, C. A., S.-C. C. Chiu, Z. Lawrence, P. Bodin, and S. Horton (2009), Array observations of microseismic noise and the nature of H/V in the Mississippi Embayment, *Bulletin of the Seismological Society of America*, *99*(5), 2893–2911.

Lecocq, T., C. Caudron, and F. Brenguier (2014), MSNoise, a python package for monitoring seismic velocity changes using ambient seismic noise, *Seismological Research Letters*, *85*(3), 715–726.

Li, Y.-G., J. E. Vidale, K. Aki, F. Xu, and T. Burdette (1998), Evidence of shallow fault zone strengthening after the 1992 M7. 5 Landers, California, earthquake, *Science*, *279*(5348), 217–219.

Li, Y.-G., J. E. Vidale, S. M. Day, D. D. Oglesby, and E. Cochran (2003), Postseismic fault healing on the rupture zone of the 1999 M 7.1 Hector Mine, California, earthquake, *Bulletin of the Seismological Society of America*, *93*(2), 854–869.

Li, Y.-G., P. Chen, E. S. Cochran, J. E. Vidale, and T. Burdette (2006), Seismic evidence for rock damage and healing on the San Andreas fault associated with the 2004 M 6.0 Parkfield earthquake, *Bulletin of the Seismological Society of America*, *96*(4B), S349–S363.

Liu, C., A. T. Linde, and I. S. Sacks (2009), Slow earthquakes triggered by typhoons, *Nature*, *459*(7248), 833.

Liu, C., C. A. Langston, C. A. Powell, and C. H. Cramer (2018a), Near Surface to Upper Mantle Velocity Structure in the Mississippi Embayment from Ambient Noise Tomography, *AGU Fall Meeting Abstracts*.

Liu, C., K. Aslam, and C. A. Langston (2019), Directionality of ambient noise in the mississippi embayment, *EarthArXiv, doi: 10.31223/osf.io/5q8hx*.

Liu, Z., J. Huang, P. He, and J. Qi (2018b), Ambient noise monitoring of seismic velocity around the Longmenshan fault zone from 10 years of continuous observation, *Journal of Geophysical Research: Solid Earth*, *123*(10), 8979–8994.

Meier, U., N. M. Shapiro, and F. Brenguier (2010), Detecting seasonal variations in seismic velocities within Los Angeles basin from correlations of ambient seismic noise, *Geophysical Journal International*, *181*(2), 985–996.

Minato, S., T. Tsuji, S. Ohmi, and T. Matsuoka (2012), Monitoring seismic velocity change caused by the 2011 Tohoku-Oki earthquake using ambient noise records, *Geophysical Research Letters*, *39*(9).

Murnaghan, F. D. (1951), *Finite deformation of an elastic solid*, Wiley.

Nishimura, T., N. Uchida, H. Sato, M. Ohtake, S. Tanaka, and H. Hamaguchi (2000), Temporal changes of the crustal structure associated with the M6.1 earthquake on September 3, 1998, and the volcanic activity of Mount Iwate, Japan, *Geophysical Research Letters*, *27*(2), 269–272.

Niu, F., P. G. Silver, T. M. Daley, X. Cheng, and E. L. Majer (2008), Preseismic velocity changes observed from active source monitoring at the Parkfield SAFOD drill site, *Nature*, *454*(7201), 204.

Ohmi, S., K. Hirahara, H. Wada, and K. Ito (2008), Temporal variations of crustal structure in the source region of the 2007 Noto Hanto earthquake, central Japan, with passive image interferometry, *Earth, planets and space*, *60*(10), 1069–1074.

Peng, Z., and Y. Ben-Zion (2006), Temporal changes of shallow seismic velocity around the Karadere-Düzce branch of the north Anatolian fault and strong ground motion, *Pure and Applied Geophysics*, *163*(2-3), 567–600.

Poupinet, G., W. Ellsworth, and J. Frechet (1984), Monitoring velocity variations in the crust using earthquake doublets: An application to the Calaveras Fault, California, *Journal of Geophysical Research: Solid Earth*, *89*(B7), 5719–5731.

Rivet, D., F. Brenguier, and F. Cappa (2015), Improved detection of preeruptive seismic velocity drops at the piton de la fournaise volcano, *Geophysical Research Letters*, *42*(15), 6332–6339.

Rubinstein, J. L., and G. C. Beroza (2004a), Evidence for widespread nonlinear strong ground motion in the Mw 6.9 Loma Prieta earthquake, *Bulletin of the Seismological Society of America*, *94*(5), 1595–1608.

Rubinstein, J. L., and G. C. Beroza (2004b), Nonlinear strong ground motion in the ML 5.4 Chittenden earthquake: Evidence that preexisting damage increases susceptibility to further damage, *Geophysical research letters*, *31*(23).

Rubinstein, J. L., N. Uchida, and G. C. Beroza (2007), Seismic velocity reductions caused by the 2003 Tokachi-Oki earthquake, *Journal of Geophysical Research: Solid Earth*, *112*(B5).

Sabra, K. G., P. Gerstoft, P. Roux, W. Kuperman, and M. C. Fehler (2005), Surface wave tomography from microseisms in Southern California, *Geophysical Research Letters*, *32*(14).

Schaff, D. P., and G. C. Beroza (2004), Coseismic and postseismic velocity changes measured by repeating earthquakes, *Journal of Geophysical Research: Solid Earth*, *109*(B10).

Sens-Schönfelder, C. (2008), Synchronizing seismic networks with ambient noise, *Geophysical Journal International*, *174*(3), 966–970.

Sens-Schönfelder, C., and E. Larose (2008), Temporal changes in the lunar soil from correlation of diffuse vibrations, *Physical Review E*, *78*(4), 045,601.

Sens-Schönfelder, C., and U. Wegler (2006), Passive image interferometry and seasonal variations of seismic velocities at Merapi Volcano, Indonesia, *Geophysical research letters*, *33*(21).

Shapiro, N. M., and M. Campillo (2004), Emergence of broadband Rayleigh waves from correlations of the ambient seismic noise, *Geophysical Research Letters*, *31*(7).

Silver, P. G., T. M. Daley, F. Niu, and E. L. Majer (2007), Active source monitoring of cross-well seismic travel time for stress-induced changes, *Bulletin of the Seismological Society of America*, *97*(1B), 281–293.

Stehly, L., M. Campillo, and N. Shapiro (2006), A study of the seismic noise from its long-range correlation properties, *Journal of Geophysical Research: Solid Earth*, *111*(B10).

Stehly, L., M. Campillo, and N. Shapiro (2007), Traveltime measurements from noise correlation: stability and detection of instrumental time-shifts, *Geophysical Journal International*, *171*(1), 223–230.

Tanimoto, T., S. Ishimaru, and C. Alvizuri (2006), Seasonality in particle motion of microseisms, *Geophysical Journal International*, *166*(1), 253–266.

Tian, Y., and M. H. Ritzwoller (2015), Directionality of ambient noise on the Juan de Fuca plate: Implications for source locations of the primary and secondary microseisms, *Geophysical Journal International*, *201*(1), 429–443.

Tsai, V. C. (2011), A model for seasonal changes in GPS positions and seismic wave speeds due to thermoelastic and hydrologic variations, *Journal of Geophysical Research: Solid Earth*, *116*(B4).

Wang, Q.-Y., F. Brenguier, M. Campillo, A. Lecointre, T. Takeda, and Y. Aoki (2017), Seasonal crustal seismic velocity changes throughout Japan, *Journal of Geophysical Research: Solid Earth*, *122*(10), 7987–8002.

Weaver, R., B. Froment, and M. Campillo (2009), On the correlation of non-isotropically distributed ballistic scalar diffuse waves, *The Journal of the Acoustical Society of Amer-*

*ica*, *126*(4), 1817–1826.

Weaver, R. L., and O. I. Lobkis (2001), Ultrasonics without a source: Thermal fluctuation correlations at Mhz frequencies, *Physical Review Letters*, *87*(13), 134,301.

Wegler, U., and C. Sens-Schönfelder (2007), Fault zone monitoring with passive image interferometry, *Geophysical Journal International*, *168*(3), 1029–1033.

Wegler, U., B.-G. Lühr, R. Snieder, and A. Ratdomopurbo (2006), Increase of shear wave velocity before the 1998 eruption of Merapi volcano (Indonesia), *Geophysical Research Letters*, *33*(9).

Withers, M. M., R. C. Aster, C. J. Young, and E. P. Chael (1996), High-frequency analysis of seismic background noise as a function of wind speed and shallow depth, *Bulletin of the Seismological Society of America*, *86*(5), 1507–1515.

Wu, C., A. Delorey, F. Brenguier, C. Hadziioannou, E. G. Daub, and P. Johnson (2016), Constraining depth range of s wave velocity decrease after large earthquakes near Parkfield, California, *Geophysical Research Letters*, *43*(12), 6129–6136.

Yamamura, K., O. Sano, H. Utada, Y. Takei, S. Nakao, and Y. Fukao (2003), Long-term observation of in situ seismic velocity and attenuation, *Journal of Geophysical Research: Solid Earth*, *108*(B6).

Yang, Y., M. H. Ritzwoller, A. L. Levshin, and N. M. Shapiro (2007), Ambient noise Rayleigh wave tomography across Europe, *Geophysical Journal International*, *168*(1), 259–274.

Young, I. (1999), Seasonal variability of the global ocean wind and wave climate, *International Journal of Climatology: A Journal of the Royal Meteorological Society*, *19*(9), 931–950.

Zhan, Z., V. C. Tsai, and R. W. Clayton (2013), Spurious velocity changes caused by temporal variations in ambient noise frequency content, *Geophysical Journal International*, *194*(3), 1574–1581.

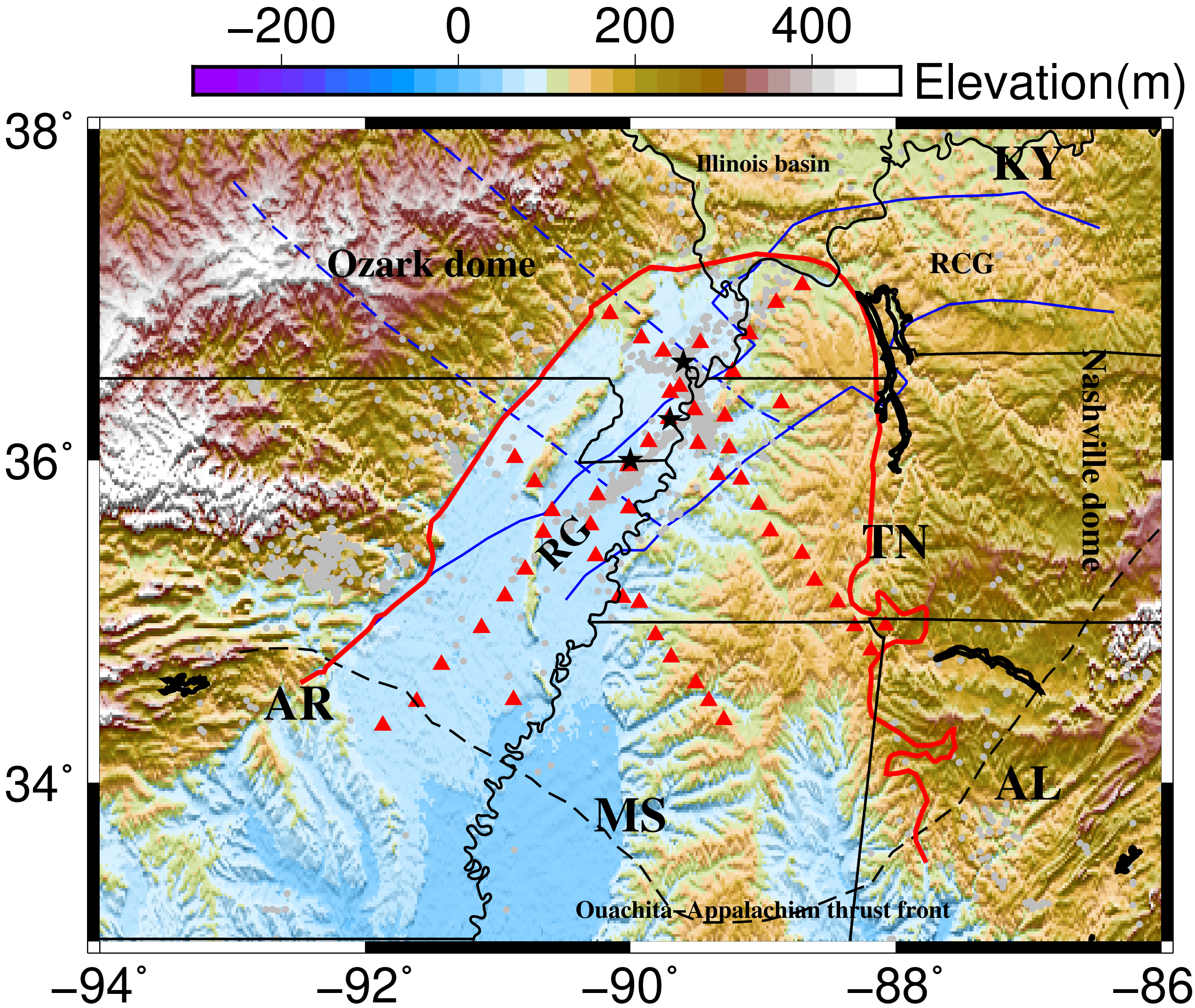


**Figure 1.** Index map of the Mississippi embayment in the central United States showing $M_w > 2.0$ earthquake catalog from 1990 to present (small gray dots), three $M_w > 7.0$ earthquakes (black stars), broadband stations (red triangles) used for CCs, Reelfoot-Rough Creek graben (RG-RCG, blue solid lines) and Missouri Batholith (blue dashed lines) modified from *Hildenbrand and Hendricks* [1995], sediment boundaries of Mississippi embayment (red solid lines) modified from *Dart* [1992] and *Dart and Swolfs* [1998], Ouachita-Appalachian thrust front (black dashed lines), Nashville dome and Ozark dome. From southwest to northeast, three major earthquakes occurred on Dec.16, 1811 with $M_w = 7.7$, Jan. 23, 1812 with $M_w = 7.5$, and Feb. 7, 1812 with $M_w = 7.7$.

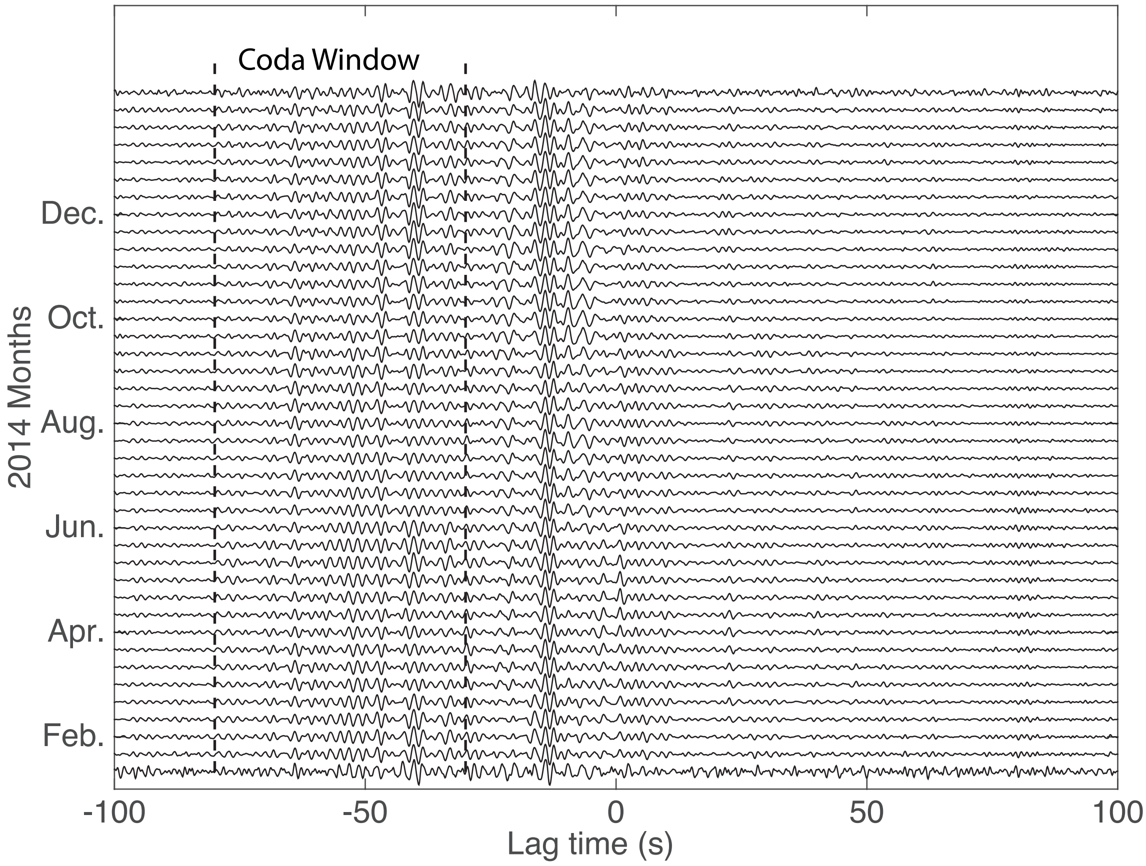


**Figure 2.** Example of 30 days moving stacked vertical component CCs for the station pair C07:C08 of the network NELE in 2014. The interstation distance is 30 km. The CCs are in the passband of 0.3-1 Hz. The dashed lines from -80 s to -30 s mark the coda window.

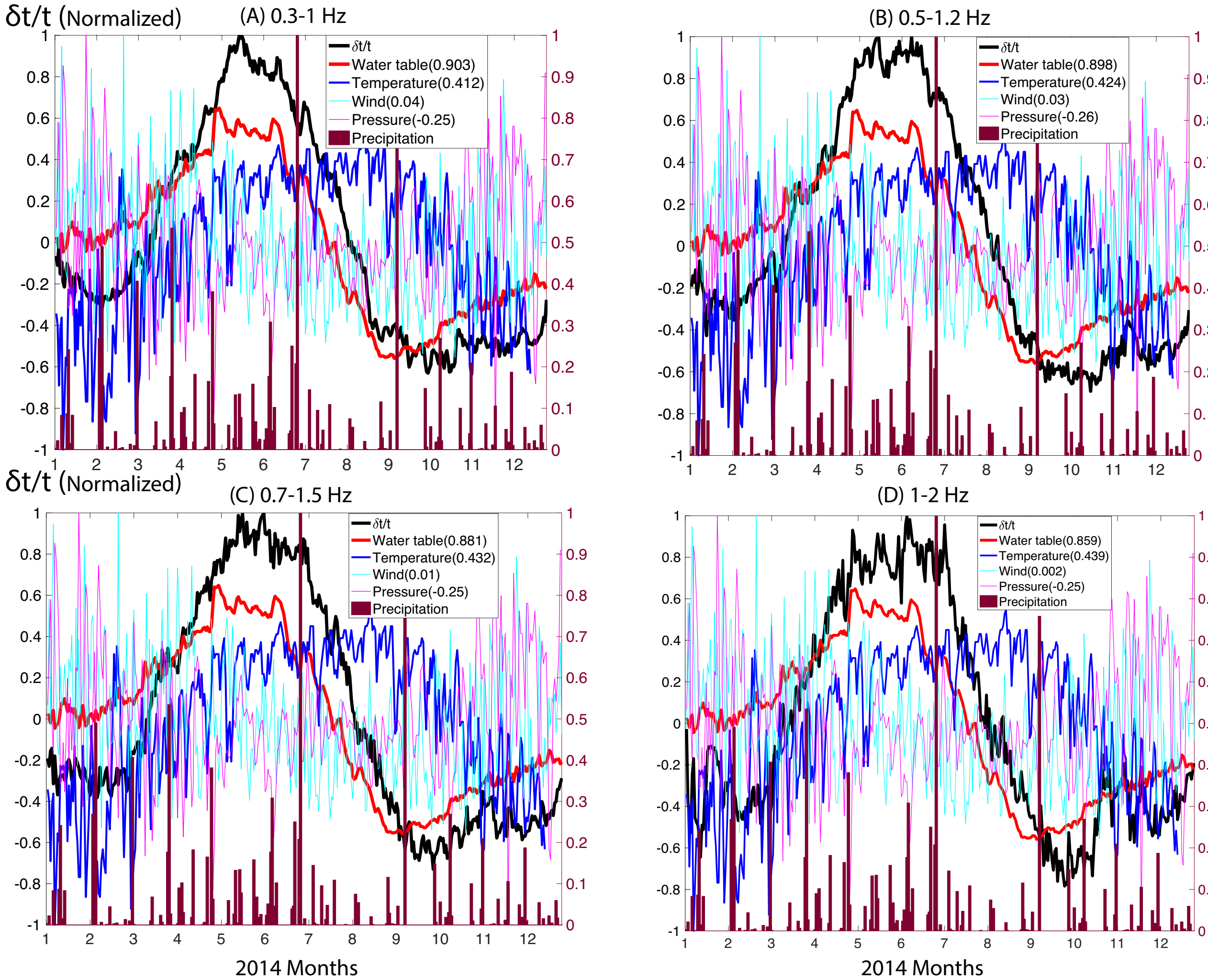


**Figure 3.** The correlation of averaged normalized $\delta t/t$ for all station pairs with normalized climatological parameters, water table fluctuation, precipitation, temperature, wind speed, and atmospheric pressure, in the passbands from 0.3-1, 0.5-1.2, 0.7-1.5, and 1-2 Hz. The right-side vertical scale is for the normalized precipitation. The values after the climatological parameters in the legend represent the correlation coefficients with the $\delta t/t$. The $\delta t/t$ correlates primarily with the normalized water table fluctuation in all predefined frequency ranges. No clear relationship could be observed between the normaized $\delta t/t$ and wind speed, precipitation and atmospheric pressure. As *Tsai* [2011] and *Hillers et al.* [2015a] suggested, temperature changes should be positively correlated with the $\delta v/v$ variations which is opposite to what we observe.

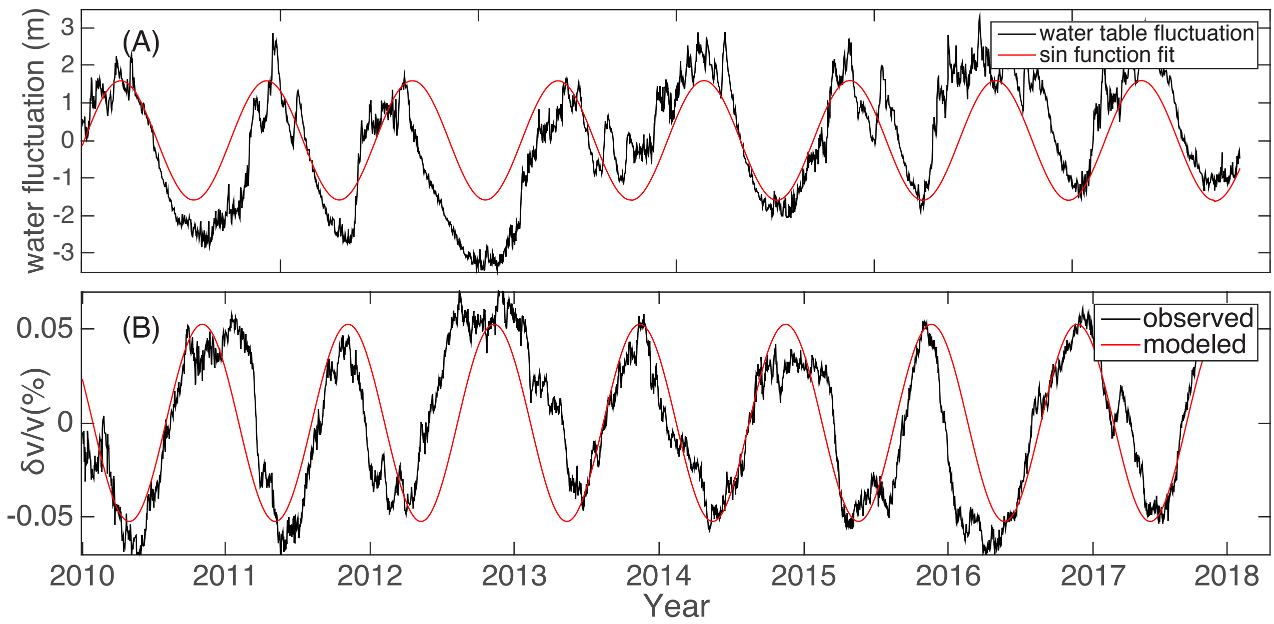


**Figure 4.** Comparison of modeled and observed $\delta v/v$ from the poroelastic solution. (A) We approximate the true water table fluctuation (black), which varies from year to year, with an averaged sinusoidal fit (red). This is necessary because the water fluctuation and $\delta v/v$ are slightly phase shifted due to the diffusion effect, thus we cannot use the true water table level directly in the model calculations. (B) Comparison between the observed $\delta v/v$ (black) and model predictions (red) assuming $m/\mu = -2000$. This value is within the range of values inferred from laboratory observations of the nonlinear elastic properties of rock.

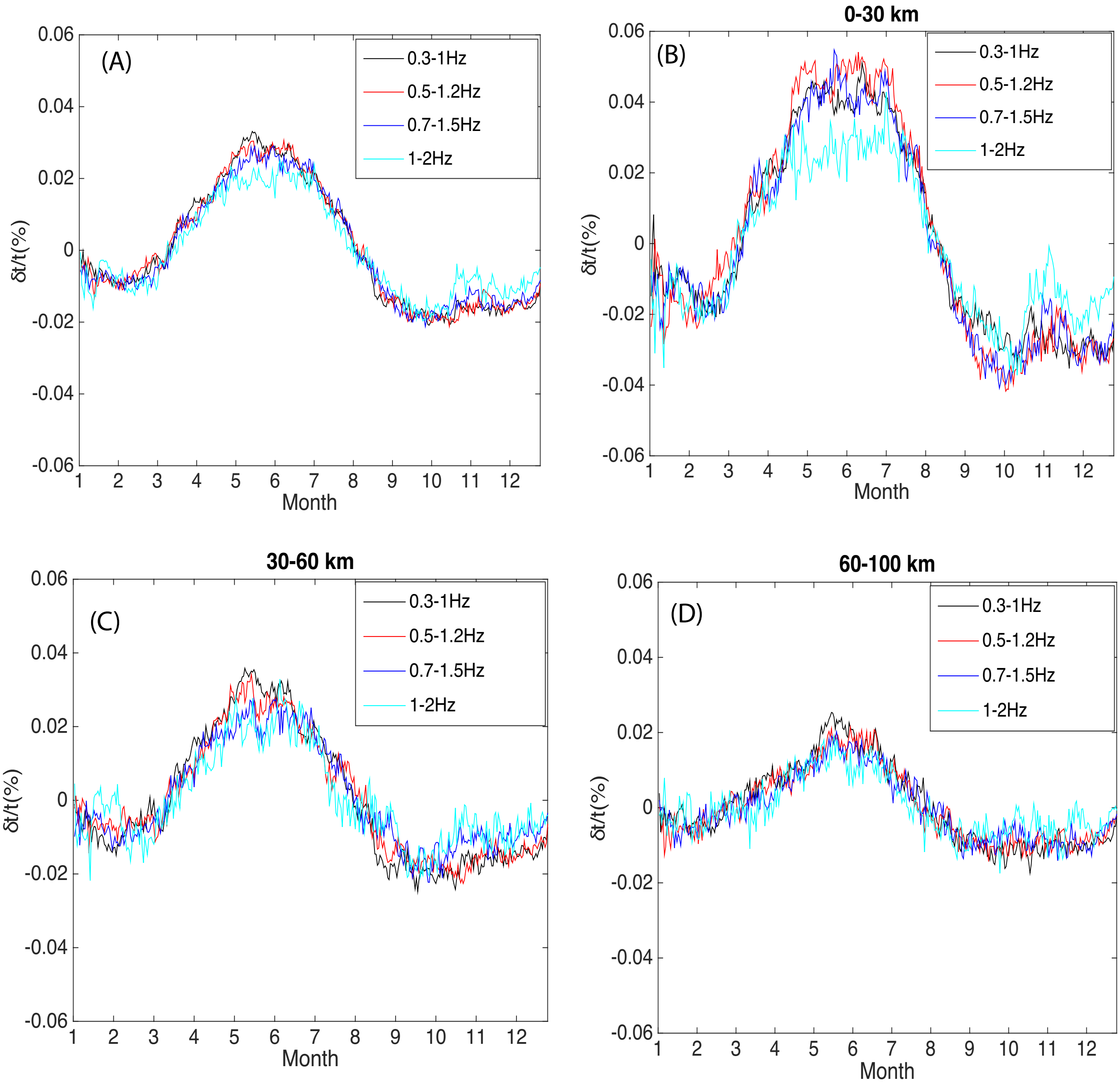


**Figure 5.** The average velocity change in different frequency bands for different interstation distances. (A) Average velocity change for all station pairs with interstation distance between 0 and 100 km in 4 predefined frequency ranges, 0.3-1, 0.5-1.2, 0.7-1.5, and 1-2 Hz. The maximum $\delta t/t$ decreases from 0.03% in the passband of 0.3-1 Hz to 0.02% in the 1-2 Hz. (B-D) $\delta t/t$ variations in different distance ranges. Maximum $\delta t/t$ variations decrease with increasing frequency and interstation distance.

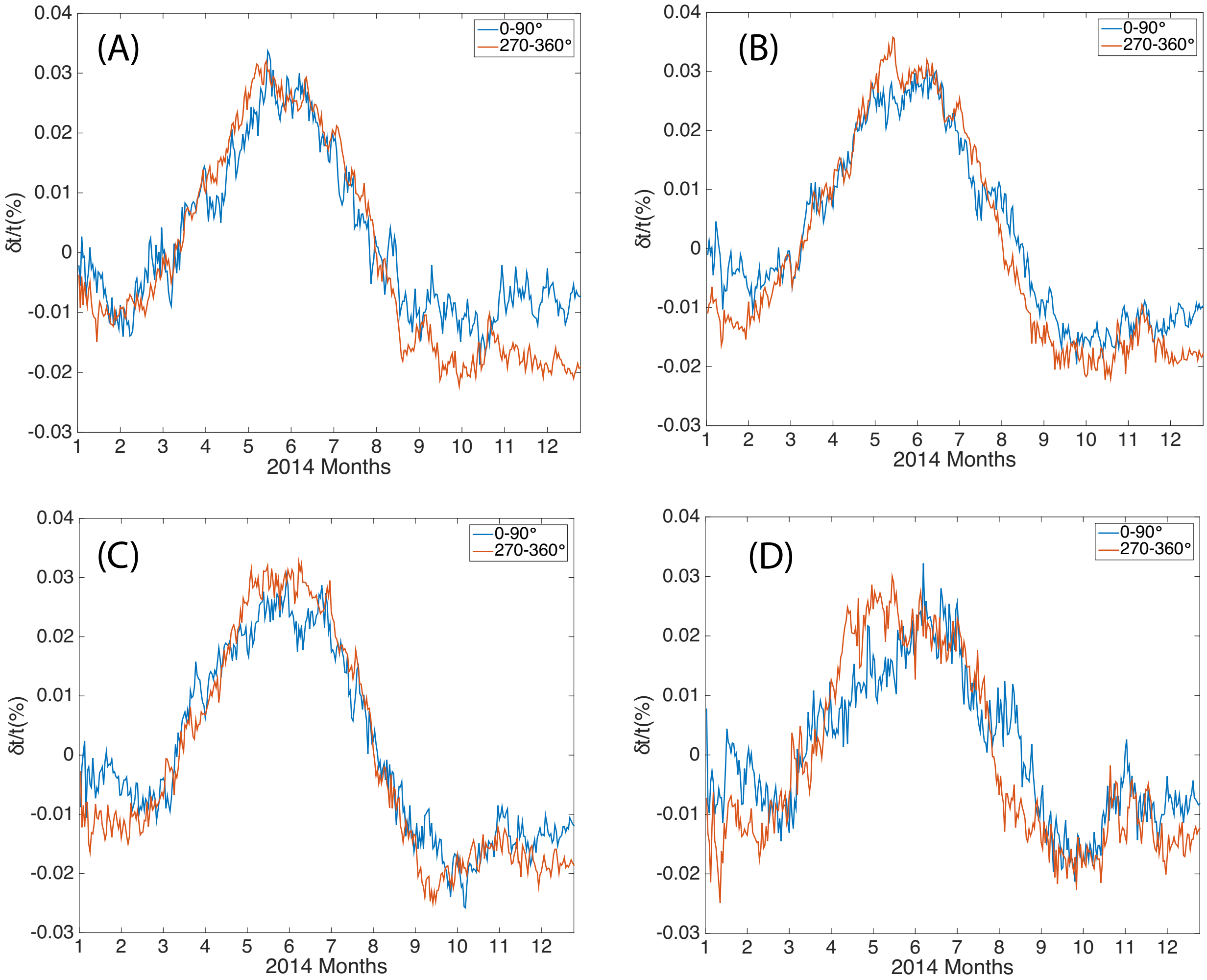


**Figure 6.** $\delta t/t$ dependence on the azimuth in the passband of 0.3-1 Hz, 0.5-1.2 Hz, 0.7-1.5 Hz, and 1-2 Hz. Average $\delta t/t$ variations in the azimuth of 0-90° and 270-360° are similar to each other, and the differences between them are small. The non-uniform distribution of noise sources has a small effect on the $\delta t/t$ variations.

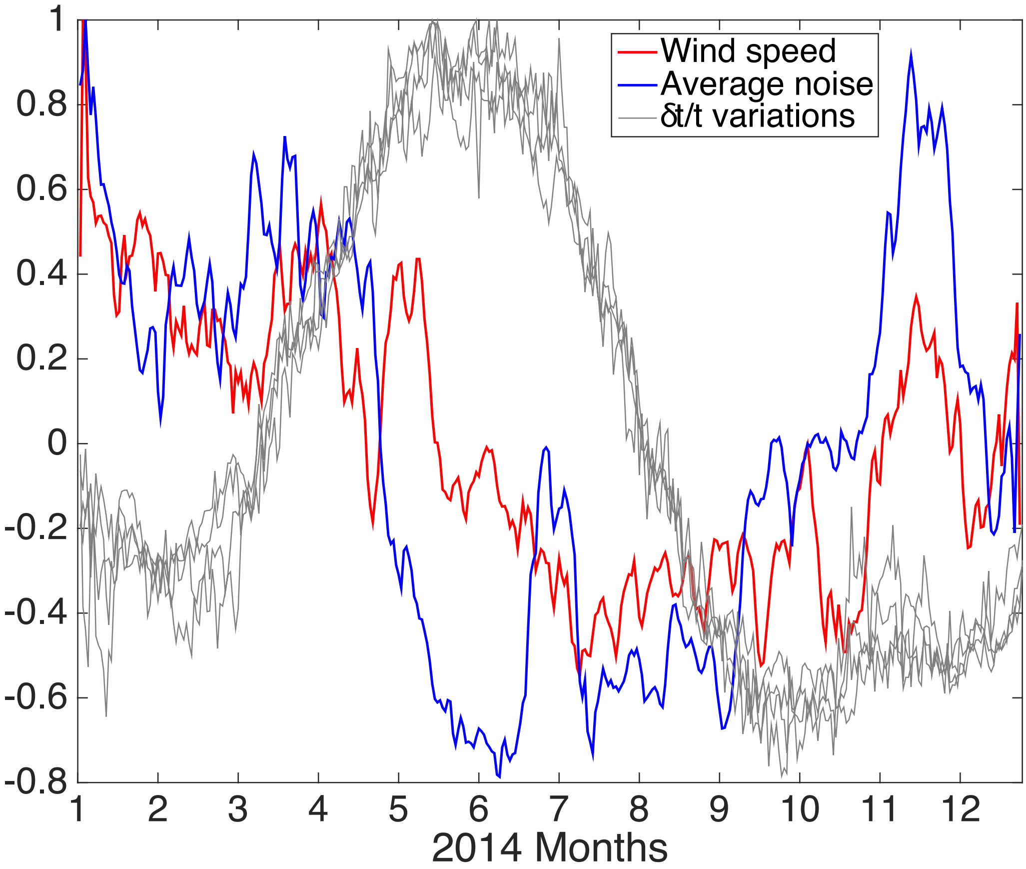


**Figure 7.** $\delta t/t$ dependence on the seasonal variation of noise amplitude. High similarity, though not an exact match, can be observed between seasonal variation of noise amplitude and wind speed, which suggests the noise in the passband of 0.3-2 Hz could be composed of oceanic microseisms, induced surface waves, and wind noise. High similarity can be observed between the variations of noise amplitude and $\delta t/t$ from January to April and October to December. A large increase of noise amplitude induces a small increase of $\delta t/t$ in November, which suggests that noise amplitude may introduce a small bias into the velocity measurements. The bias from noise amplitude variation is small compared to the maximum velocity change induced from the water table fluctuation from April to September. We suggest that the velocity variations are primarily related to the pore pressure changes in the crust or sediments, rather than the seasonal variations of the ambient noise amplitude.

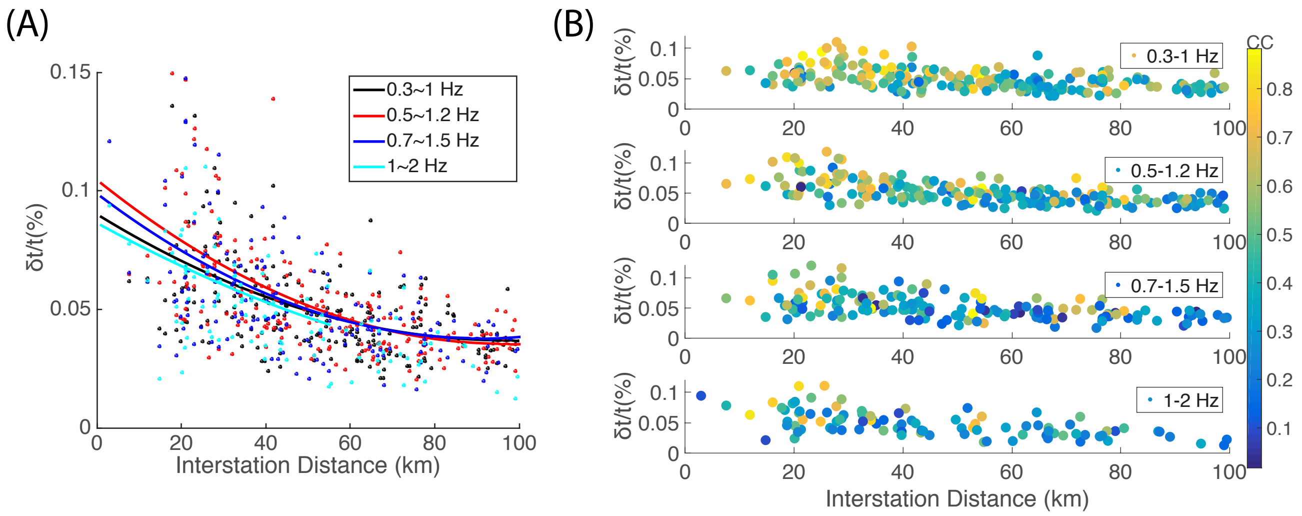


**Figure 8.** $\delta t/t$ and correlation coeffcient dependence on the interstation distance. (A) The maximum $\delta t/t$ variations decrease non-linearly with the interstation distance. At close distance, $\delta t/t$ samples a small region and holds a wide range of values, which could be related to local sediment structure. At larger distances, $\delta t/t$ samples a large region so that it tends to stabilize to an average value. (B) Correlation coefficient dependence on the distance and frequency. The correlation coefficients are between water table fluctuation and $\delta t/t$ variations. High coefficients ($> 0.6$ ) may be observed more often in the passband of 0.3-1 Hz than 1-2 Hz because high-frequency coherent noise attenuates faster than low-frequency noise.